

High-Frequency Concurrent Measurements in Watershed and Impaired Estuary Reveal Coupled DOC and Decoupled Nitrate Dynamics

Gopal K. Mulukutla¹ · Wilfred M. Wollheim^{1,2} · Joseph E. Salisbury³ · Richard O. Carey⁴ · Thomas K. Gregory³ · William H. McDowell²

Received: 16 January 2021 / Revised: 1 May 2021 / Accepted: 24 May 2021 / Published online: 10 June 2021 © Coastal and Estuarine Research Federation 2021

Abstract

Rapid changes in land use, pollution inputs, and climate are altering the quantity, timing, and form of materials delivered from watersheds to estuaries. To better characterize these alterations simultaneous measurements of biogeochemical conditions in watersheds and estuaries over a range of times scales are needed. We examined the strength of watershed-estuarine biogeochemical coupling using in situ measurements of nitrate, terrestrial dissolved organic carbon (DOC), and chloride collected over a 7-month period in a nitrogen-impaired estuary in northeastern US. The watershed exerted strong control over concentrations of terrestrially derived DOC in the estuary, attributable to relative homogeneity of watershed sources from forested land combined with relatively conservative behavior in estuarine waters. Estuarine nitrate patterns were more complex, suggesting the influence of heterogeneous watershed distribution of non-point and point sources and high reactivity of nitrate in the estuary. Understanding estuarine biogeochemical patterns will be advanced through greater use of simultaneous sub-hourly measurements of inflows, salinity, and water quality in estuaries and their upstream watersheds.

Keywords Water quality · Watershed-estuary biogeochemical coupling · Eutrophication

Communicated by Dennis Swaney

Key Points

- Simultaneous water quality measurements in watershed and N-impaired estuary show strong watershed control for estuarine DOC but complex coupling for nitrate.
- DOC exhibited near-conservative behavior in the estuary.
- For nitrate, spatial distribution of watershed sources and interactions with internal estuarine processes produce complex response.
- Gopal K. Mulukutla gopal.mulukutla@unh.edu
- Earth Systems Research Center, University of New Hampshire, Durham, NH, USA
- Department of Natural Resources and the Environment, University of New Hampshire, Durham, NH, USA
- Ocean Processes Analysis Laboratory, University of New Hampshire, Durham, NH, USA
- Massachusetts Department of Environmental Protection, Worcester, MA, USA

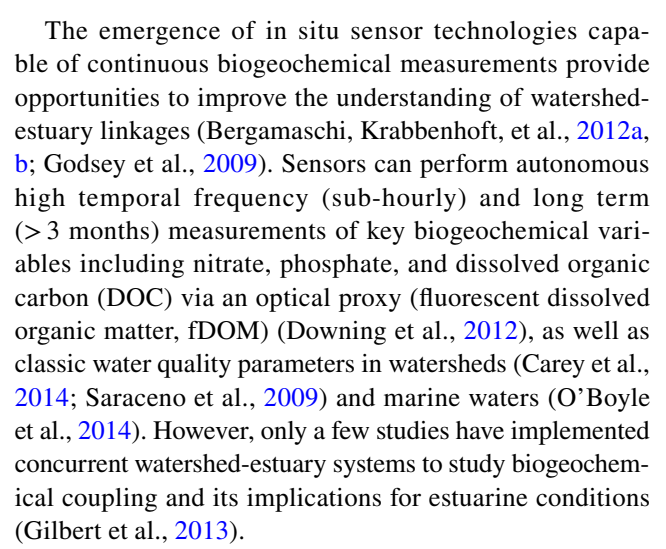
Introduction

Estuaries are strongly influenced by inputs of freshwater, nutrients, and carbon from coastal watersheds. The degree of influence is determined by several factors that can vary over space and time, including magnitude and frequency of storms, estuarine residence time relative to watershed area, the degree of anthropogenic activity, and consequent changes in land use composition (Arndt et al., 2007; Pinckney et al., 2001; Salisbury et al., 2008; Swaney et al., 2008). Eutrophication of estuarine waters due to nitrogen (N) enrichment is increasing, causing many problems such as loss of biodiversity, increased algal blooms, hypoxic water, acceleration of species invasions, and shifts in dominant biogeochemical pathways (Barbier et al., 2011; McClelland & Valiela, 1998; Smyth et al., 2013; Wetz & Yoskowitz, 2013). Watershed inputs of dissolved organic carbon (DOC) to coastal areas is also occurring, potentially impacting light regimes and food webs (Balch et al., 2016). As a result, the ability of estuaries to provide the many important benefits of healthy ecosystems is continuing to decline (Deegan et al., 2012; Grabowski & Peterson, 2007).



Human activities alter the amount and timing of nutrient and organic matter inputs delivered to estuaries (Bowen & Valiela, 2008). Both watershed drivers and estuarine responses are further influenced by factors such as climate change and associated changes in temperature, sea levels, wind patterns, and the hydrologic cycle (Bricker et al., 2008; Salisbury et al., 2009; Statham, 2012). Increases in anthropogenic N and changes to organic matter fluxes are occurring in many watersheds due to expanding agriculture, urbanization, and associated land use change. Although much anthropogenic N is retained in watersheds (Boyer et al., 2002) increased loading leads to increased export through rivers and streams (Seitzinger & Kroeze, 1998). Estuaries modulate exports of DOC (and other forms of carbon) with high in situ production rates, and spatial and temporal heterogeneity (Bauer et al., 2013). This has resulted in studies that report near-conservative behavior of DOC in some estuaries (Mantoura & Woodward, 1983; Vallino et al., 2005), but non-conservative behavior in others (McKenna, 2004). Laboratory studies show that terrestrial DOC can be highly reactive due to "salting out" or microbial degradation (Battin et al., 2009; Moran et al., 1999; Schlesinger & Bernhardt, 2013). Furthermore, hydrologic conditions can strongly influence the mobilization, transport, and retention of nutrients and carbon within watersheds (Coble et al., 2019; Kaushal et al., 2014; Morse & Wollheim, 2014). Thus, with climate change, the controlling mechanisms of estuarine conditions will also likely change.

Watershed-estuary coupling can occur continuously during periods of baseflow or episodically during stormflow. An estuary responds to watershed and environmental drivers over multiple temporal scales (Cloern & Nichols, 1985): (a) short duration driven by daylight or tides; (b) storm event scale, driven by freshwater inflows lasting hours to weeks; (c) seasonal, due to changes in precipitation, temperature, and watershed function; and (d) annual, that incorporate longer term climate oscillations and trends. Previous estuarine studies focused on seasonal or annual time scales that combined infrequent observations of biogeochemical characteristics (e.g., weekly or monthly) with finer temporal scale observations of inflows (Clair et al., 2013; Valiela & Bowen, 2002). However, a focus on broader time scales limits understanding of estuarine responses at finer time scales (Bergamaschi, Fleck, et al., 2012a, b; Bergamaschi, Krabbenhoft, et al., 2012a, b; Robins et al., 2018). For example, during storms, patterns in N concentration exported from watersheds may exhibit increase, decrease, or remain chemostatic with flow, depending on watershed or time period (Godsey et al., 2009). Estuarine storm response may or may not reflect watershed patterns due to complicated circulation, stratification, or strong biological activity. Knowledge of these patterns often requires simultaneous sub-daily measurements in both watershed and estuary.



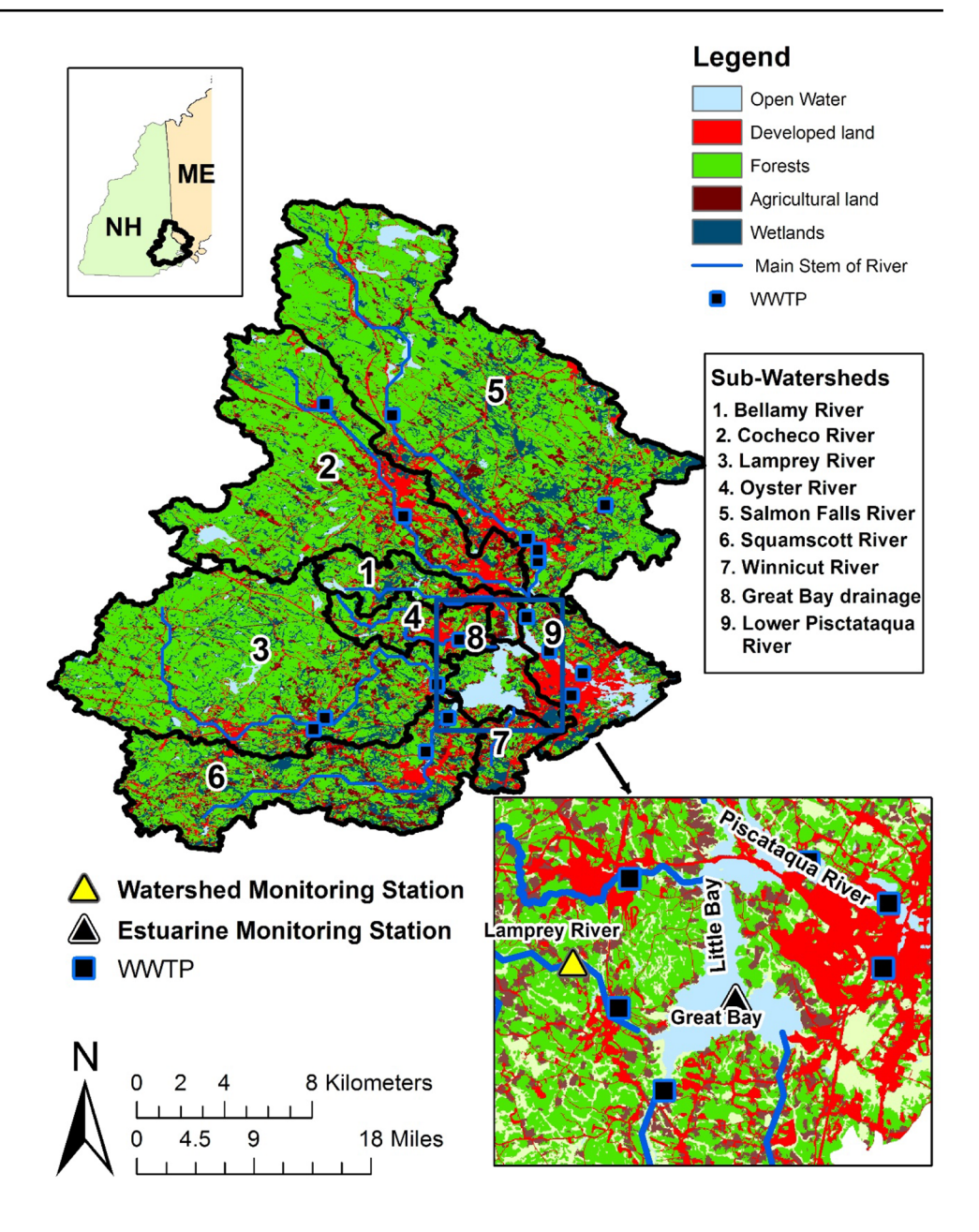
The objective of this study was to examine seasonal and storm event dynamics of estuarine nitrate and DOC using simultaneous measurements of river and estuarine chemistry. We conducted this study in Great Bay, New Hampshire, USA, and in the watershed of its largest tributary, Lamprey River. This estuary system faces long-term land-use change and increasing climate variability. We hypothesized that (a) storm-event watershed nitrate and DOC fluxes will provide greater control on corresponding estuarine concentrations and that the estuary will show minimal coupling (biogeochemical response in the estuary attributable to watershed inflows of water and dissolved constituents) during baseflow; (b) due to the spatial homogeneity of watershed sources, estuarine DOC will respond more to storm-event watershed DOC fluxes than estuarine nitrate to nitrate fluxes; and (c) for both nitrate and DOC, monitoring in one sub-watershed will not be fully representative of variability observed in estuarine conditions.

Study Site and Methods

The Great Bay estuary is located in northeastern USA (Fig. 1). The estuary system consists of nine major subwatersheds formed by seven major tributaries (Table 1). The watershed (2651 km²) has a population of 400,000 people living in 55 urbanizing municipalities (Mills, 2009; Trowbridge et al., 2014). The estuarine system is strongly tidal with relatively shallow morphology marked by limited vertical stratification (Short, 1992), a large volume relative to inputs, and a baseflow residence time of 13–20 days (Text S1, supporting information). Great Bay is showing signs of eutrophication attributed mainly to nitrogen over-enrichment from both point (32%) and non-point sources (68%) (PREP, 2013). Increased N loads in recent years (Bresler, 2012; Trowbridge, 2010) have



Fig. 1 Map of Great Bay watershed showing land use, wastewater treatment plants (WWTP), sub-watersheds, sub-estuaries, and water quality monitoring stations. Refer to Table 1 for summary land-use statistics



contributed to greater prevalence of phytoplankton and nuisance macroalgae, and leading the US-EPA to list it as N-impaired with regulations proposed such as expensive upgrades to wastewater treatment plants (WWTP). Increased storm activity in the region (Douglas et al., 2011) has also increased inputs of terrestrial DOC and turbidity to coastal waters (Balch et al., 2016). Excess nutrients and associated issues, along with factors such as reduced water clarity and light penetration, have contributed to drastic declines in the acreage of eelgrass, the estuary's cornerstone vegetation (Beem & Short, 2009). Focus of this study is Great Bay proper, the largest sub-estuary

in the estuarine system, and the Lamprey River sub-watershed (Fig. 1).

Measurements

Continuous, high-frequency (every 30 min) measurements of nitrate, fDOM, and conductance/salinity were made using in situ sensors deployed simultaneously in the estuary and its tributary, the Lamprey River (Figs. 1 and 2). Sensors were deployed for one growing season (May–November 2011). A detailed description of the instrumentation used is given in supporting information



Table 1 Land use statistics for the Great Bay w	watershed and its major sub-watersheds
--	--

Watershed	Total area (km²)	Developed land (km²) (%)	Agricultural land (km²) (%)	Forests and wetlands (km²) (%)	Water (km ²) (%)	Remarks
Great Bay	2652.5	369.9 (14.0)	202.5 (7.6)	1976.6 (74.5)	103.4 (3.9)	Whole watershed
Bellamy River	87.9	16.7 (19.0)	8.7 (9.8)	58.2 (66.2)	4.4 (5.0)	
Cocheco River	479.8	74.4 (15.5)	34.5 (7.2)	359 (74.8)	12 (2.5)	
Lamprey River	555.0	55.8 (10.1)	32.7 (5.9)	456.3 (82.2)	10.3 (1.9)	Sub-watershed monitored in this study
Oyster River	79.1	17.7 (22.4)	9.1 (11.5)	50.5 (63.9)	1.8 (2.3)	
Salmon Falls River	852.6	84.5 (9.9)	57.8 (6.8)	686.1 (80.5)	24.2 (2.8)	
Squamscott/Exeter River	330.6	47.7 (14.4)	40.1 (12.1)	239 (72.3)	3.9 (1.2)	
Winnicut River	48.1	14.0 (29.2)	5.2 (10.8)	28.3 (58.7)	0.7 (1.4)	
Great Bay Drainage	70.6	10.6 (15.0)	6.7 (9.5)	30.3 (43.0)	23 (32.5)	Direct drainage to Great Bay proper
Lower Piscataqua Drainage	147.4	48.5 (32.9)	7.7 (5.2)	67.9 (46.0)	23.3 (15.8)	Direct drainage to Piscataqua River

(Section SI0 and Table S0). River flow data was obtained from a co-located discharge gage operated by the US Geological Survey (#01073500 Lamprey River near Newmarket, NH). A linear regression between weekly grab measurements (DOC, NO₃, and Cl) and corresponding sensor variable (fDOM, NO₃, specific conductance) was used to correct sensor measurements. Instantaneous watershed fluxes were estimated at a given instant of time, f(t), as:

$$f(t) = C(t) \times Q(t) \tag{1}$$

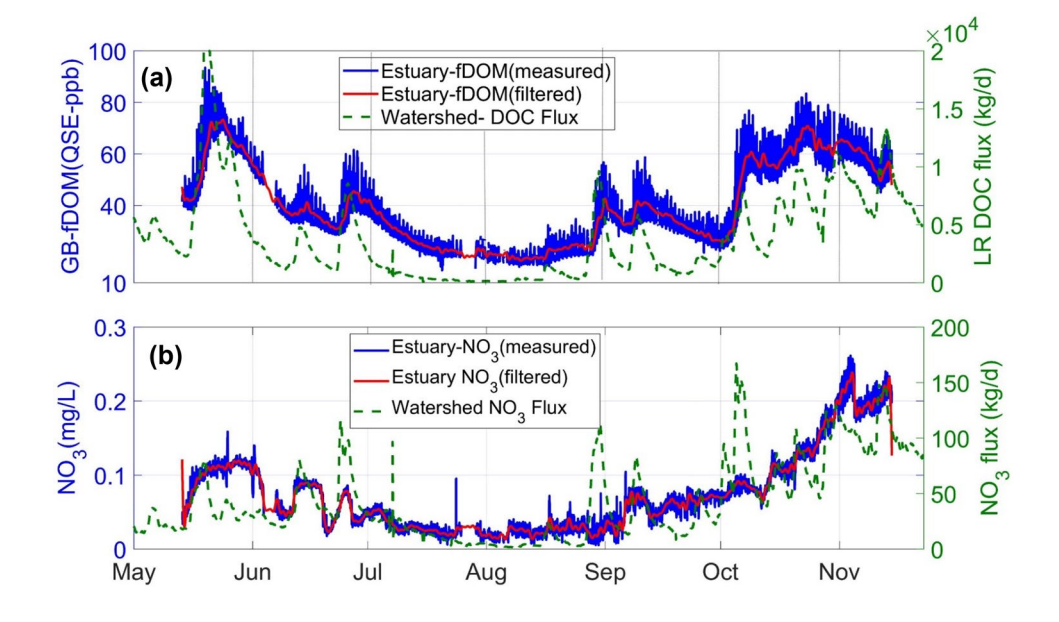
where C(t) (M L⁻³) is the measured concentration of the constituent and Q(t) (L³ T⁻¹) is the flow across the river at time instant t.

Data Analysis Methods

Data Pre-Processing

Individual time series obtained for both monitoring locations (estuarine and riverine) contained measurements aggregated to an hourly interval. These variables were first quality controlled by eliminating outliers. Segments of data with data were linearly interpolated to remove any missing data and make the time series temporally continuous, a pre-condition for the application of time series techniques described below. For the estuarine measurements, tidal influences on the time series of variables were removed using a low-pass filter (Johnson et al., 2006). According

Fig. 2 (a) Time series of estuarine fDOM and watershed DOC fluxes from the Lamprey River in 2011. fDOM is reported in quinine sulfate equivalents parts per billion units (QSE ppb). (b) Time series of estuarine nitrate concentrations and watershed nitrate fluxes. Filtered signal refers to removal of tide dominant frequencies





to this procedure, the Fourier transform of the signal was first computed. The amplitude of spectral frequencies higher than 1.375 cycles per day were zeroed to remove the dominant semi-diurnal component. The signal was then reconstructed through an inverse Fourier transform. The reconstructed signal developed by applying this technique contains only the weaker tidal frequencies along with any variability caused by diel biological processing.

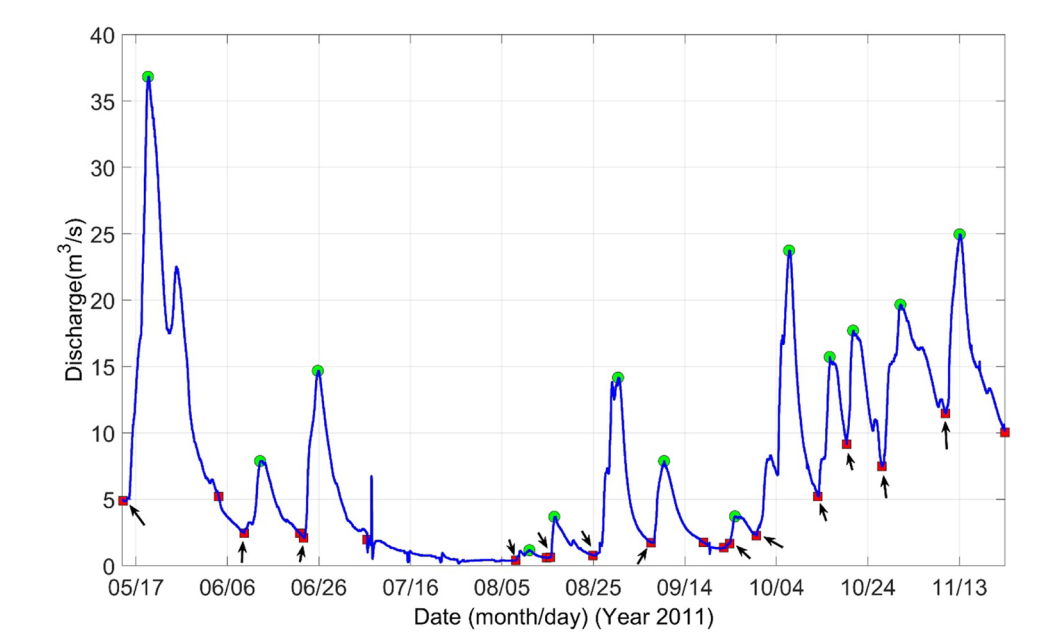
Time Series Methods

We applied frequency-dependent coherence (C; 0 < C < 1), a time series analysis technique, to evaluate how estuarine concentrations (NO₃, fDOM, and Cl) vary over time in conjunction with a related watershed variable (freshwater inflows; NO₃, DOC, and Cl concentration and fluxes). Given two time series u(t) and v(t) frequency-dependent coherence within a narrow band of frequency ($\Delta\omega$) with center at ω_0 is given as (Menke & Menke, 2012)

$$C_{uv}^{2}(\omega_{0}, \Delta\omega) = \frac{\left|\tilde{u}^{*}(\omega_{0})\tilde{v}(\omega_{0})\right|^{2}}{\left|\tilde{u}(\omega_{0})\right|^{2}\left|\tilde{v}(\omega_{0})\right|^{2}}$$
(2)

where $\tilde{u}(\omega_0)$ and $\tilde{v}(\omega_0)$ are the Fourier transforms of u(t) and v(t), at frequency ω_0 , respectively, and $\tilde{u}^*(\omega_0)$ is the Fourier transform of time reversed u(t), at frequency ω_0 . The coherence profile is constructed by applying Eq. (2) over the entire frequency range of a signal. Coherence values reported here are denoted by subscripted variable \overline{C}_{E-R} , where overbar represents an average coherence over a given time period and E and R represent (filtered) the estuarine constituent concentration and watershed variable, respectively.

Fig. 3 Discharge hydrograph for the Lamprey River with delineated storm events. Square (red) marker with black arrow indicates baseflow condition at the beginning of a storm event. Plain square markers indicate end of a storm event where it was possible to distinguish from the beginning of the next storm event. Round (green) markers indicate peak flow during an event. Additional variations in flow observed during summer dry period are attributed to water releases from an upstream reservoir



Storm Event Delineation

We examined individual storm event patterns between estuarine concentrations and watershed nutrient fluxes (hysteresis) to determine intra-storm watershed-estuary coupling. These patterns are analogous to the cyclical concentration-discharge relationships that develop when solute concentrations at a particular discharge rate differ during the rising and falling limb of storm hydrographs in watershed studies (Carey et al., 2014; Evans & Davies, 1998). Such studies have been used to gain insights into many processes, including relative contribution of preferential delivery (source or transport limitation) of water and nutrients (Camporese et al., 2014; Dusek & Vogel, 2016; Lloyd et al., 2016; Phillips, 2003), and complex catchment responses (Williams, 1989). We analyzed 13 freshwater storm events for the influence of freshwater discharge, DOC, and NO₃ fluxes on estuarine concentration patterns. River flow data was obtained from a discharge gage operated by the US Geological Survey (site id 01,073,500, Lamprey River near Newmarket, NH).

Each storm was partitioned by 3 points: the start of the storm (beginning of rising limb), peak flow (beginning of falling limb), and end of the storm (termination of falling limb). The beginning of a storm event was identified based on a minimum flow increase of 1.5 m³ s⁻¹ (see Fig. 3). The end of storm was determined by identifying the earliest point since the beginning of a storm that was within 0.5 m³ s⁻¹ of observed baseflow. Some storm events constituted two or more high flow points, a consequence of a lull followed by more precipitation. For this study, such events were identified as a single storm event with highest among the multiple high flows identified as peak storm flow. Also, the beginning of the increase in flow identified for the earliest peak and the



end of the flow identified for the latest peak were selected as the beginning and end of the storm event, respectively (Fig. 3).

Storm characteristics examined include overall estuarine concentration response (increase/decrease), rotational pattern (clockwise/anti-clockwise/multi-loop), and degree of coupling between watershed and estuary where degree of storm event-scale coupling is defined using a power-law function, $P = b F^{\alpha}$, where P is the estuarine constituent concentration, F is the watershed flux of a given constituent, b is a constant of proportionality, and α is a fitted parameter (Basu et al., 2010; Godsey et al., 2009). We applied this to individual rising and falling limbs of storm-event watershed inputs. An α (estuarine responsiveness) that is positive indicates increased estuarine concentrations resulting from storm inputs. A zero or non-significant exponent indicates no coupling, while a negative exponent indicates declining concentrations resulting from storm inputs (Table 2).

Results

Watershed and Estuarine Biogeochemical Patterns

Estuarine fDOM tracks well with watershed DOC fluxes (Fig. 2a), with a pattern of high concentrations observed during high runoff in spring and autumn (~60 quinine sulfate equivalent parts per billion (QSE-ppb)) and lower

concentrations during summer low flows (~30 QSE-ppb). Terrestrial DOC is the major portion of observed fDOM response (4.04 QSE-ppb recorded at salinity of 32 psu). Through the rest of this discussion fDOM will be used interchangeably with "terrestrial DOC". Each storm event peak in DOC flux is followed closely by a peak in fDOM. Watershed NO₃ fluxes and estuarine NO₃ concentrations (Fig. 2b) also show high levels in late spring and fall (0.1–0.2 mg NL⁻¹), and lows in the summer (<0.05 mg NL⁻¹). But in contrast to fDOM, estuarine NO₃ concentrations show less pronounced response to storm-event flows (Fig. 2b).

Partitioning response time scales provided by coherence analysis allows insights into watershed-estuary coupling. *Frequency-dependent coherence* response of each estuarine constituent (Cl, fDOM, NO₃ concentrations) was examined by pairing initially with watershed discharge (Fig. 4a) and then with respective watershed concentrations (Fig. 4b) and flux (Fig. 4c). Given that river discharge varies over several orders of magnitude while concentrations of most constituents are less variable in the Lamprey River (Coble et al., 2019; Koenig et al., 2017), we would expect that coherence between estuarine concentrations and watershed fluxes would be stronger than coherence between estuary and watershed concentrations.

Over the study period using time scales greater than 1 day the average coherence of estuarine constituent concentrations was highest when related to watershed discharge (Table 3), with all three constituents exhibiting

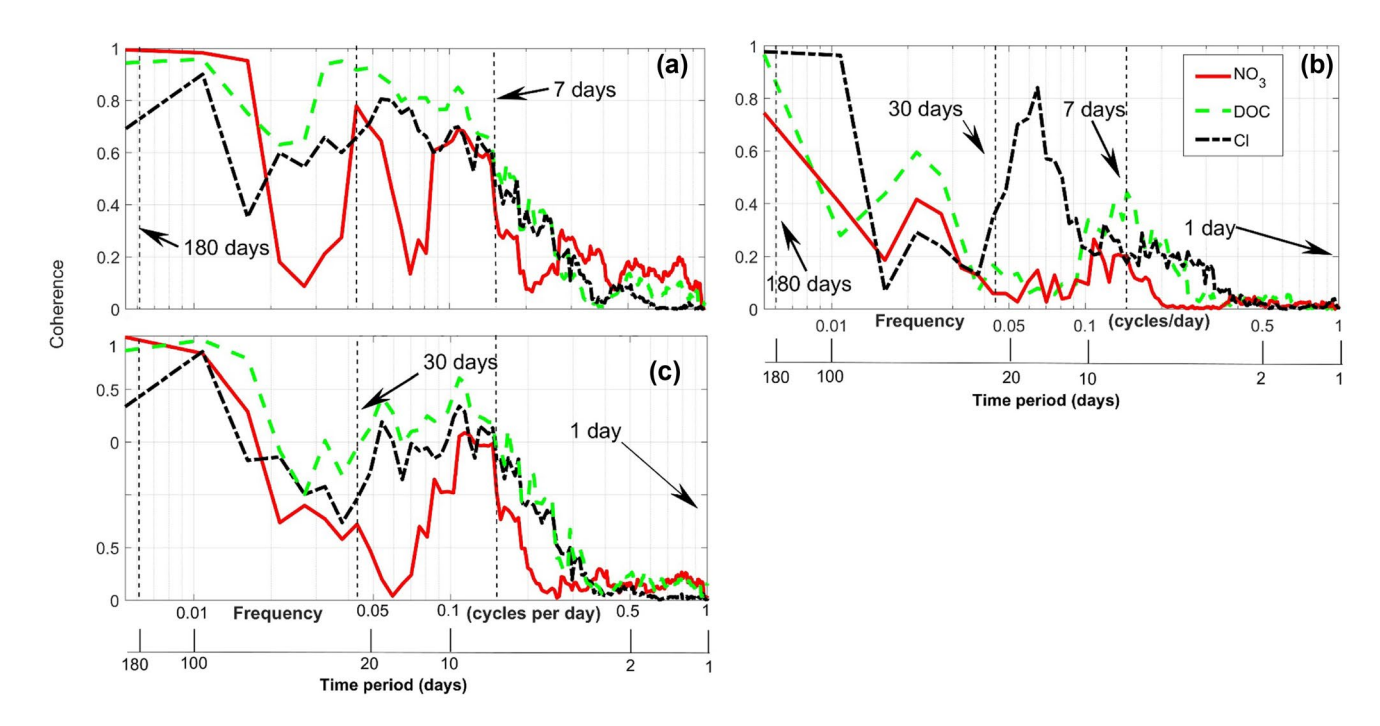


Fig. 4 Frequency-dependent coherence between estuarine NO₃, fDOM, and chloride with **(a)** watershed discharge, **(b)** respective watershed concentrations (NO₃, fDOM, and chloride), and **(c)** respec-

tive watershed fluxes (NO₃, DOC and chloride). Data is plotted in frequency domain, alternate time axis also shown with some time scales of interest highlighted in plot



similar levels of coherence ($\overline{C}_{NO3-Q}=0.21$, $\overline{C}_{fDOM-Q}=0.22$, $\overline{C}_{Cl-Q}=0.17$). Coherence was much lower when relating estuarine concentrations with watershed concentrations ($\overline{C}_{NO3-NO3}=0.05$, $\overline{C}_{fDOM-DOC}=0.09$, $\overline{C}_{Cl-Cl}=0.11$) (Fig. 4b). Coherence between estuarine DOC and Cl and corresponding watershed DOC and Cl fluxes were similar to those when using discharge, while coherence between estuarine NO₃ and watershed NO₃ fluxes was lower than when using discharge ($\overline{C}_{NO3-NO3flux}=0.13$, $\overline{C}_{fDOM-DOCflux}=0.21$, $\overline{C}_{Cl-Clflux}=0.16$).

Over long time scales (> 100 days) coherences were high between estuarine fDOM, NO₃, and Cl and corresponding watershed constituent fluxes (Fig. 4c; $\overline{C}_{NO3-NO3flux}=0.99$, $\overline{C}_{fDOM-DOCflux}=0.95$, $\overline{C}_{Cl-Clflux}=0.73$) indicating the predominant role of freshwater inputs over seasonal time scales. Likewise, coherences between concentrations and fluxes over short time scales (< 6 days) are very low ($\overline{C}_{NO3-NO3flux}=0.07$, $\overline{C}_{fDOM-DOCflux}=0.11$, $\overline{C}_{Cl-Clflux}=0.07$), suggesting that the watershed has minimal influence over estuarine variability over these time scales.

At intermediate time scales (6–30 days), a time span that encompasses storm flows (Table 2), the response of estuarine concentrations to watershed fluxes for all three constituents was observed to be intermediate in magnitude. Coherence between estuarine concentrations and watershed flux was much greater than when using watershed concentration across all time scales (Fig. 4b) and were similar or lower than when using discharge (Fig. 4a). When watershed inputs of freshwater are large enough relative to the volume of the estuary, it will depress estuarine Cl levels within those time scales, and exhibit high values of coherence.

When using watershed fluxes, NO₃ coherence was lower than DOC or Cl across all time scales, and especially during intermediate scales (Fig. 4c). For both Cl and DOC, there is a broad peak approached by around 7 days (Fig. 4c) with declines occurring around 20 days. Average duration of storm events examined here is 11.3 days (and a median duration of 12 days), suggesting that time period of greatest coherence in the Cl signals is directly a result of freshwater flows into the estuary. In contrast, NO₃ coherence also peaks around 7-9 days but the decline occurs much earlier and rapidly at around 15 days, suggesting a divergence in behavior compared to Cl. Average coherence during this period is greater for DOC than for NO₃ ($\overline{C}_{fDOM-DOCflux} = 0.67$, $C_{NO3-NO3flux} = 0.38$). The observed response at intermediate time scale is a collective indication of watershed inputs from all storm events and the differences in NO₃ and DOC with Cl warrant further examination.

These results suggest that over the course of the year flows drive variability in estuarine concentrations, while changes in watershed concentrations are secondary. Although coherence with discharge was similar or better when using watershed fluxes, we chose constituent fluxes as the basis for further study because in principle they should provide better coherence and because time scales where this is not true may be informative.

Storm Event Patterns

In our examination of storm-event patterns in estuarine concentration vs. watershed fluxes, some hysteresis naturally occurs due to the spatial separation between watershed and estuarine monitoring locations. Consequently, the peak/minimum in the estuarine variable occurs after the peak/minimum in the watershed variable. We did not correct the data for such lags. However, where it could be characterized lags were found to not affect our results (section S2, supporting information).

The estuarine hysteresis response observed over the whole period of deployment (Fig. 5) is a superposition of loops organized by season with the estuary responding positively to increased watershed fluxes. In contrast, individual storm response is complex as shown in hysteresis plots in the supporting information (Figures S1–S13). Further analysis revealed that storms generally modify estuarine conditions from the pre-storm state for each constituent (Fig. 2), but the strength of response varies with constituent, storm size, and time of year. Initial conditions, just prior to a storm event, for nitrate and DOC show a strong positive correlation with watershed fluxes, while Cl shows a strong negative correlation (Fig. 6) (DOC: $R^2 = 0.79$, NO_3 : $R^2 = 0.87$, C1: $R^2 = 0.72$; all p < 0.05). Storms generally tend to increase fDOM and NO3 and reduce Cl (salinity) in the estuary. fDOM and Cl hysteresis patterns (Table 2) show consistent, anti-clockwise, and clockwise response, respectively, with only two low-intensity storms showing changes in rotational pattern. NO₃ hysteresis patterns are more complex, with 6 of 13 storms recording a multi-loop pattern (Fig. 5c and Figures S1-S13, supporting information). Responsiveness (α) for NO₃ along the rising limb did not show a significant relationship with storm runoff ($R^2 = 0.05$; p > 0.05), precipitation amount $(R^2 = 0.12; p > 0.05)$, or rising limb duration $(R^2 = 0.07;$ p > 0.05) (Fig. 7a–c). However, all but two storms show a net concentrating response on the rising limb ($\overline{\alpha}_{NO3-RI}^+$ = 0.254, p < 0.05) and a weak response on the falling limb. Relatively large storms during late summer elicited only a small estuarine NO₃ response, despite the occurrence of two relatively intense events (e.g., storms 6 and 9 relative to storm 1 and 3; Table 2). Small storms of relatively short duration (6–7 days) elicited in multi-loop patterns. Several storms (storms 2, 6, 7, and 13) showed a small initial pulse in estuarine NO₃ concentration at the beginning of the rising limb.



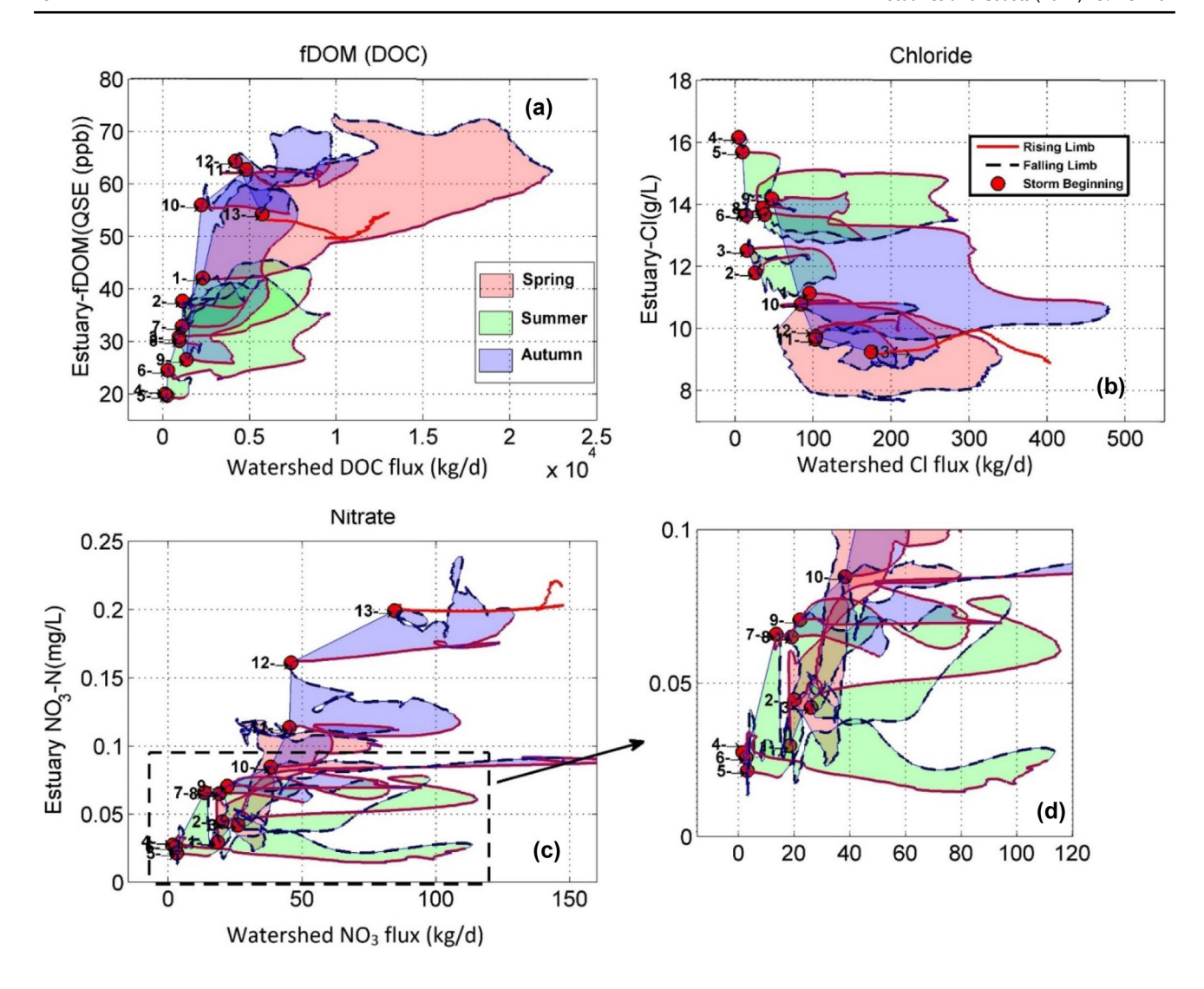


Fig. 5 Hysteresis patterns between estuarine concentrations and watershed fluxes for storm events between April and November 2011: (a) DOC, (b) Cl, (c) NO₃, and (d) inset plot showing NO₃ response

to less intense storms. Storm events are indicated at the beginning of each storm as per their description in Table 2

For fDOM the responsiveness for rising limb ($\alpha_{DOC\text{-}RL}$) showed an increase with duration (R^2 = 0.61; p < 0.05), total storm event discharge (R^2 = 0.50; p < 0.05), and total precipitation amounts (R^2 = 0.37; p < 0.05) (Fig. 8a–c) with higher responsiveness for larger storms. Corresponding results for falling limb of the storm-event were weaker. The hysteresis patterns of Cl are nearly inverse those of fDOM (Fig. 5). Five storm events (storm 2, 6, 10, 12, and 13) showed slightly increasing salinity along the rising limb ($\alpha_{Cl\text{-}RL}$ > 0) (Figures S2, S6, S10, S12, and S13). Estuarine fDOM for the same storms showed slight dilution with increasing DOC fluxes ($\alpha_{DOC\text{-}RL}$ < 0). The responsiveness pattern for Cl is weaker (Fig. 9), but clearly the opposite of fDOM response.

Discussion

Watershed Control of Estuarine DOC

For storm events, strong fDOM responsiveness was observed with multiple factors, including duration of rising limb of storm hydrograph, increased runoff, and precipitation (Fig. 8). This combined with a weaker response on the falling limb suggests that watershed-estuary connectivity is similar to hydrologic connectivity observed between watershed, and a headwater stream or river (Kaller et al., 2015; Nippgen et al., 2015). Counter to general patterns, some smaller storms resulted in increased Cl and dilution of fDOM. Tidally forced influx of ocean water through the



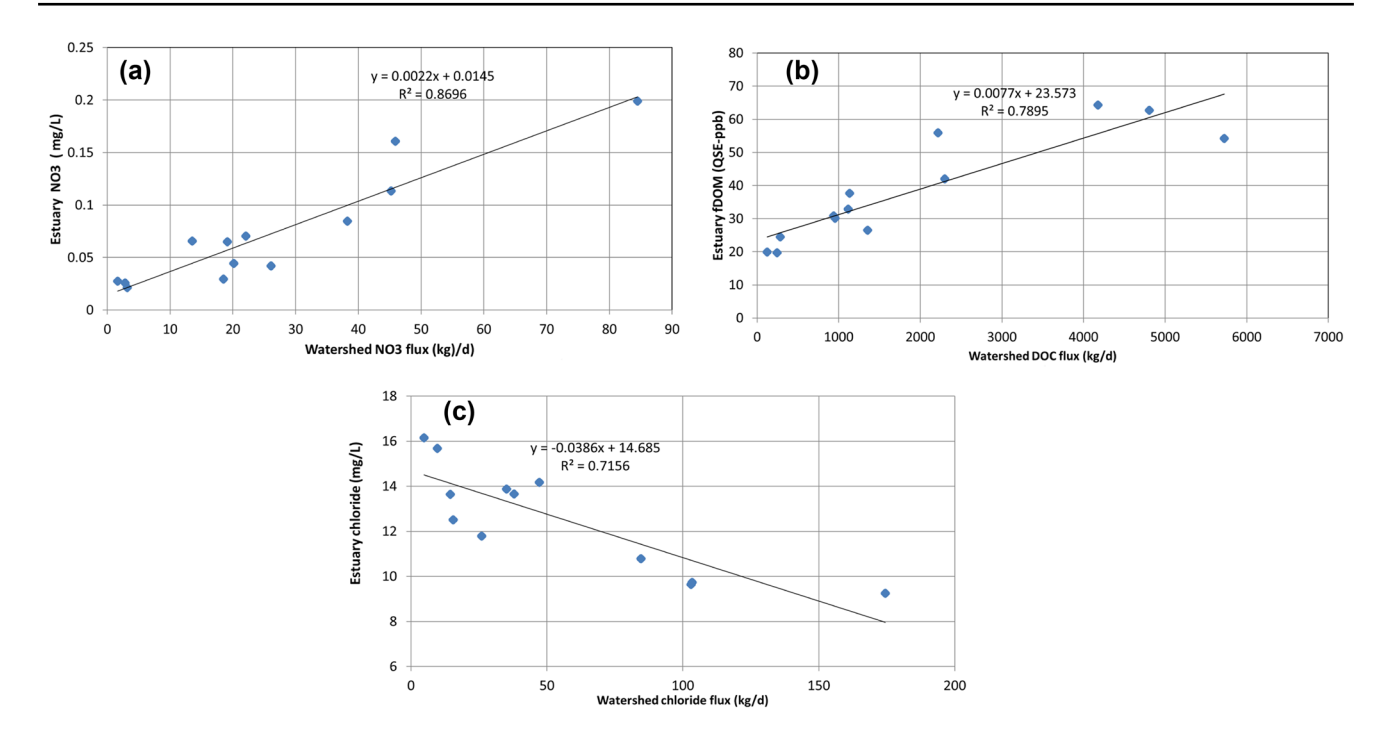


Fig. 6 Relationship between baseflow watershed fluxes just prior to beginning of a storm event and corresponding estuarine concentration: (a) NO₃, (b) estuarine fDOM and watershed DOC, and (c) chloride

estuary mouth can counter increases in terrestrial DOC inputs and cause such a dynamic (Huang et al., 2014). Also, the changing quality of DOC exported from watersheds can vary over storm events causing changes in the fDOM response (Larsen et al., 2015). However these factors were not of sufficient magnitude to confound the overall coherence response. Hysteresis analysis demonstrated the strong influence of watershed over estuarine DOC conditions over storm-event time scales (Fig. 5 and Table 2).

DOC in both freshwaters and estuaries is derived mainly from forests and wetland (Buffam et al., 2001; Creed et al., 2003). The Lamprey River sub-watershed (21% of total watershed area) consists of 82% forest and wetlands, compared to 74% for the whole watershed (Table 1). Although DOC concentrations in northeastern watersheds increase with discharge, their variability is smaller than the orders of magnitude observed in discharge variability (Raymond & Saiers, 2010). Indeed, the coherence between estuarine fDOM and discharge was just as strong as when using DOC fluxes. This leads us to conclude that the variability in terrestrial DOC captured by monitoring one sub-watershed was sufficient to explain the overall dynamics of DOC in the estuary, including inputs from unmonitored areas. As a result, watershed DOC exports may be sufficiently well predicted by commonly used, less intensive methods combining continuous flow and infrequent grab measurements.

Factors that increase runoff from watersheds will also increase DOC exported to coastal zones. This suggests that

greater watershed-estuary coupling will occur in the future when more frequent extreme events are predicted to occur (Hayhoe et al., 2007). More recently, reports indicate that terrestrial DOC is already increasing in coastal oceans in response to changing storm patterns (Balch et al., 2016). Impacts of higher fDOM in estuaries and coastal ocean include increased light attenuation and altered food webs (Traving et al., 2017). In Great Bay, eelgrass has been in decline in recent years (Beem & Short, 2009). Among the hypotheses attributed to this decline is a greater frequency of light limitation due to higher fDOM, similar to estuaries elsewhere (Ganju et al., 2014). This suggests that the changing role of watershed DOC fluxes, along with other interacting factors (e.g., suspended sediment flux and resulting turbidity), should be considered in coastal management.

Conservative Behavior of Terrestrial DOC in the Estuary

DOC and Cl coherence response is very similar in the time scale of 1–180 days. Hysteresis data provides more evidence of this similarity. Estuarine fDOM response is similar albeit nearly inverse estuarine chloride response for all storm events (Fig. 5). The inverse pattern for Cl is expected when estuarine behavior is assumed to be conservative because chloride in the estuary should decline during storms (with inflow of freshwater with less Cl than in the



Table 2 Storm characteristics and patterns between estuarine and watershed NO₃, terrestrial DOC, and Cl for 13 storm events monitored

						Estuary-fC	OM vs wa	Estuary-fDOM vs watershed DOC fluxes			Estuary No	J ₃ vs. wate	Estuary NO ₃ vs. watershed NO ₃ fluxes	fluxes		Estuary CI vs. watershed CI fluxes
Begin Storm Mean Total Total Rising date (mm- duration flow storm vol. precip. ^a limb fit, dd) (days) (m^3/s) $(m^3/10^3)$ (mm) α^c	Mean Total Total flow storm vol. precip. ^a (m^3/s) $(m^3/10^3)$ (mm)	Total Total storm vol. precip. ^a (m ³ /10 ³) (mm)	Total vol. precip. ^a (mm)	ь. а	$\begin{array}{c} Risin \\ limb \\ \alpha^c \end{array}$	ng fit,	p-Value	Falling limb fit, α ^c	p-Value	Hyst. pattern ^b	Rising limb fit, α ^c	p-Value	Falling limb fit, α ^c	p-Value Hyst.	Hyst. pattern ^b	Hyst. pattern ^b
	16.2 12,614 95	12,614 95	95		0	0.13	0.000	0.15	0.000	AC	0.51	0.000	-0.01	0.357	AC	C
12 4.5 621 56 -	4.5 621 56 -	621 56 -	- 26	1)	-0.01	0.087	0.15	0.000	AC	0.55	0.000	1.23	0.000	AC	C
14 6.6 3183 57	6.6 3183 57	3183 57	57		0	0.09	0.000	0.14	0.000	AC	0.34	0.000	90.0	0.000	ML	C
7 0.8 186 23 -	186 23	186 23	23		0	.02	0.051	-0.04	0.000	ML	-0.08	0.000	0.64	0.000	ML	ML
9 1.8 769 54	769 54	769 54	54		0.0	0	0.267	-0.07	0.000	AC	0.22	0.000	0.01	0.000	AC	C
13 5.7	5.7 3911 92	3911 92	92		0.0	9(0.000	0.07	0.000	AC	0.13	0.000	-0.15	0.000	AC	C
1303 47	1303 47	1303 47	47		0	11	0.000	0.09	0.000	AC	0.03	0.083	0.25	0.000	ML	C
6 3.1 545 38	3.1 545 38	545 38	38	·	0	-0.04	0.000	0.21	0.000	ره	-0.12	0.000	-0.11	0.000	AC	AC
13 10.6 7232 95	10.6 7232 95	7232 95	95		0	.40	0.000	0.00	0.294	AC	0.13	0.000	0.17	0.000	ML	C
6 11.5 2778 56 -	11.5 2778 56	2778 56	26		-0.0	22	0.000	-0.28	0.000	AC	0.41	0.000	0.01	0.231	ML	C
8 13.1 3507 67	13.1 3507 67	3507 67	29		0.	01	0.057	0.05	0.000	AC	0.01	0.108	-0.13	0.000	AC	C
10–27 14 15.1 7011 58 –0.02	15.1 7011 58	7011 58	. 28	•	0	.02	0.000	0.22	0.000	AC	0.11	0.000	0.29	0.000	ML	C
11–09 13 15.9 5751 69 –0.03	15.9 5751 69	5751 69	. 69 1		-0	03	0.004	NA	0.000	NA^{c}	0.10	0.000	NA	0.000	NA	NA

NA not available

^aPrecipitation recorded at nearby National Weather Service Station in Durham, NH

^bHysteresis patterns (hyst. pattern): AC anti-clockwise, C clockwise, ML multi-loop

 $^{c}\mathrm{Fit}$ parameter for equation $P\!=\!b\!\times\!F^{\alpha}$



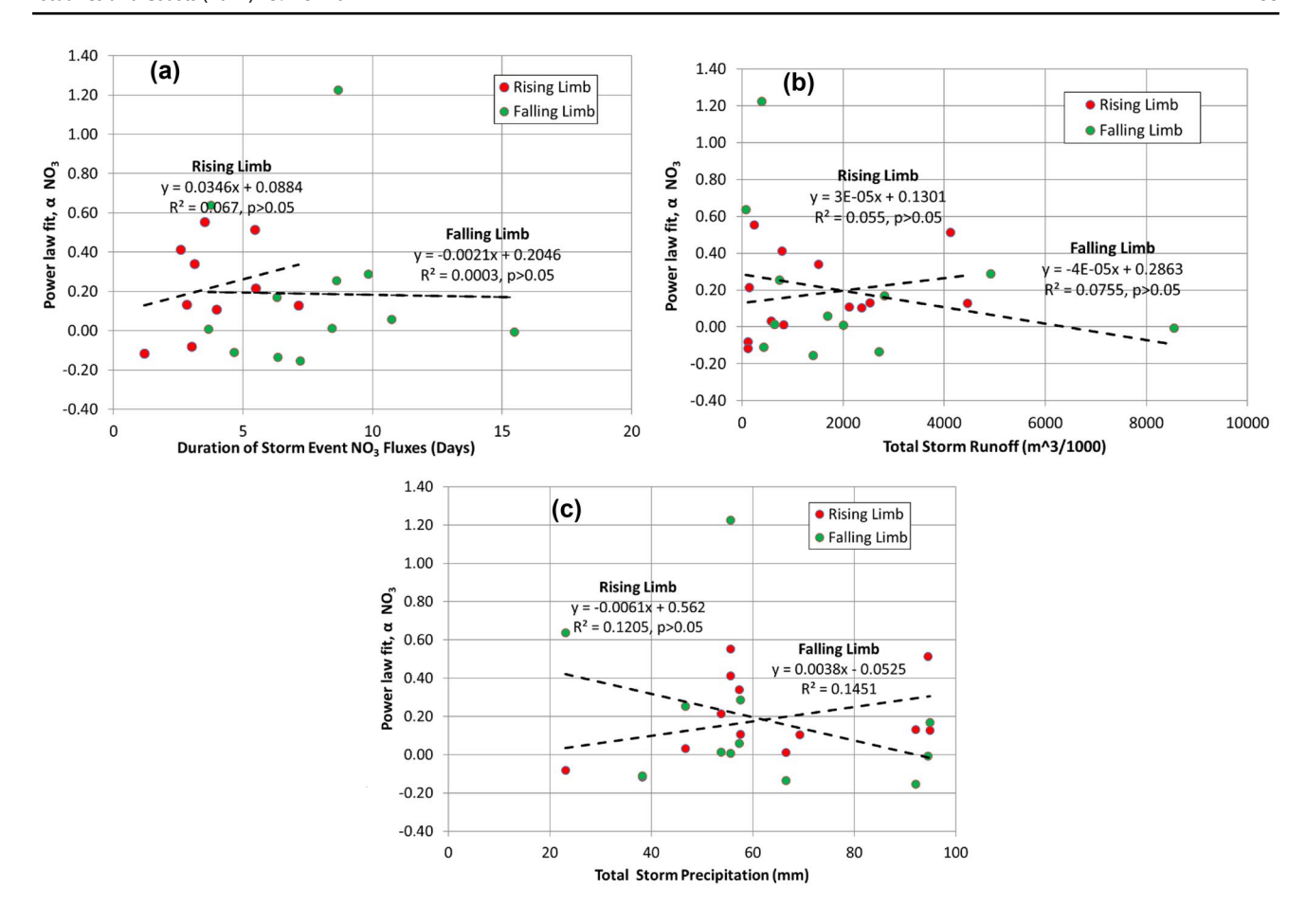


Fig. 7 Relationship between estuarine responsiveness (α) for NO₃ with (a) storm event duration, (b) total storm runoff, and (c) total storm precipitation

estuary), while fDOM in the estuary should increase (since more freshwater with more DOC than in the estuary). The fact that chloride is conservative, and the symmetrical and inverse behavior of fDOM over the 1–180-day time scale, strongly suggests that fDOM behaves in a (near-) conservative way. This behavior may be explained by the presence of simultaneous sources and sinks leading to minimal turnover within the estuary (Mantoura & Woodward, 1983) or by the removal of specific components of the DOC pool (Raymond & Spencer, 2014).

Conservative behavior of terrestrial DOC has been observed in a freshwater coastal river network of New England (Wollheim et al., 2015) as well as in larger North American river networks, unless there are long residence-time features in surface waters, such as large lakes or reservoirs (Hanley et al., 2013). Because of relatively little transformation of terrestrial DOC in the estuary, combined with the importance of transport limitation for riverine carbon transport (Bauer et al., 2013), much of this DOC may eventually make its way to the coastal ocean, as observed in the Gulf of Maine where its fate and consequence remain poorly understood (Balch et al., 2016).

Complex Behavior of Estuarine NO₃

In the Lamprey R. watershed, suburban and agricultural land cover, a major non-point source of nitrate (Wollheim et al., 2005), is 16% within this sub-watershed, and at 22% in the whole watershed. Further, anthropogenic land uses are concentrated in several of the sub-watersheds (Table 1 and Fig. 1), resulting in a heterogeneity of sources, both in the location of inputs relative to the hydrodynamic circulation within estuary and their relative influence on its condition. On annual time scales non-point N sources dominate loads of total N in the Great Bay watershed, of which a substantial portion is exported during storm events, while baseflow is dominated by point N sources (PREP, 2013). For NO₃, a focus of this study, our results provide insights into the relative importance of non-point and point N source contribution to estuarine NO₃ concentrations.

Over seasonal time scales, the coherence response is similar to that of DOC and Cl. This may be due to watershed (baseflow) influence on estuarine conditions and the predominance of point-sources over these time scales, or a simple coincidence of the periods of high and low biological activity that



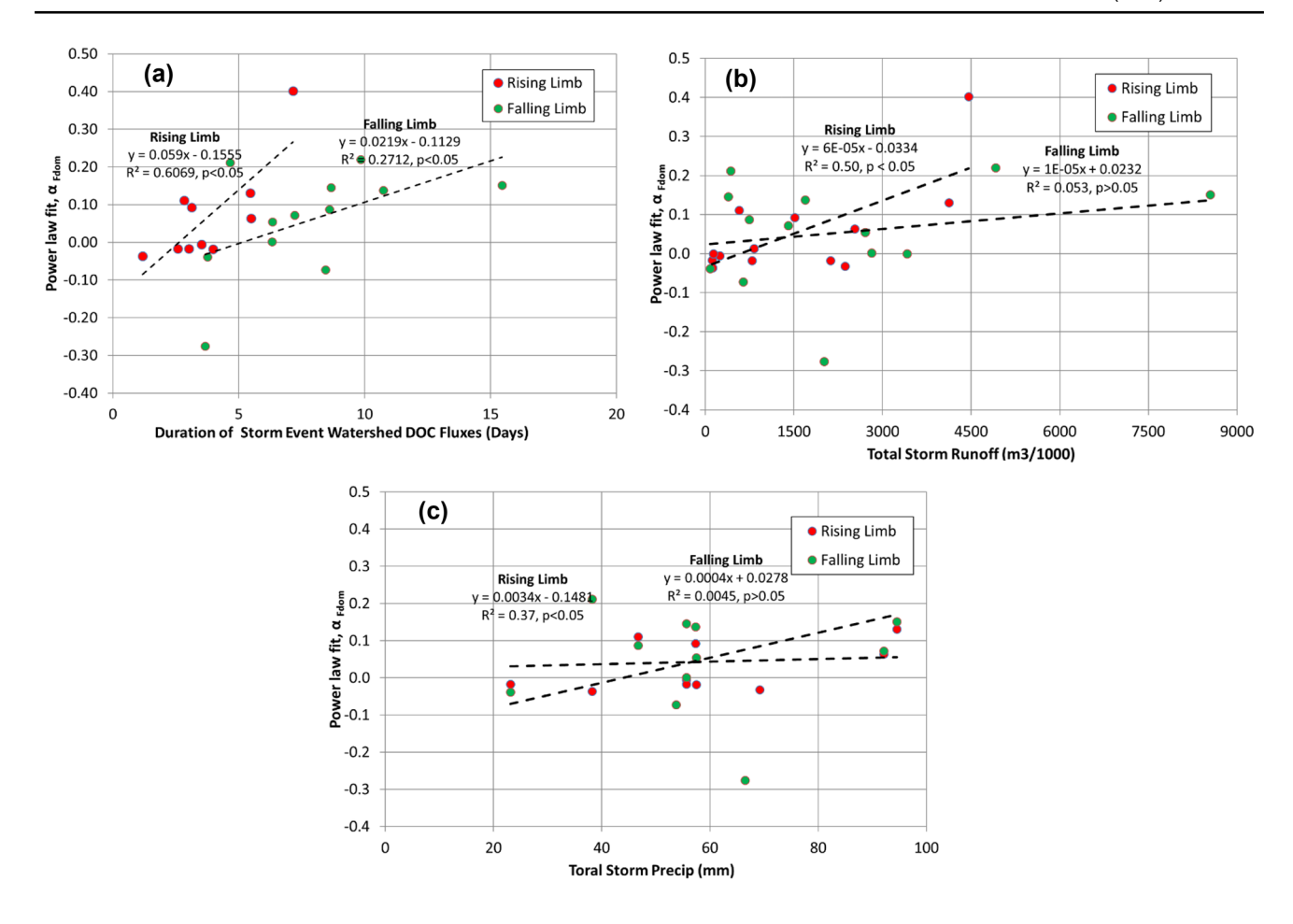


Fig. 8 Relationship between estuarine responsiveness (α) for fDOM with (a) storm event duration, (b) total storm runoff, and (c) total storm precipitation

leads to increased sources and reduced uptake occurring simultaneously in terrestrial, freshwater, and estuarine ecosystems.

If estuarine nitrate were to behave like in river systems, point-source dominant baseflow patterns would lead to dilution during storm events (Colombo et al., 2004; Jiang et al., 2014). If non-point inputs dominate, then NO₃ concentrations would increase (Feinson et al., 2016). NO₃ concentrations generally increase during storms compared to pre-storm conditions, unlike Cl which exhibits dilution. This is an important pattern as it suggests that watershed non-point sources override any dilution effect of pointsource (WWTP) and NO₃ uptake in watershed and estuary. Further evidence to this effect can be observed in the small initial pulse of nitrate observed during four events that has also been reported previously in the watershed (Carey et al., 2014), possibly a signature of non-point source inputs from developed areas downstream of the watershed monitoring station. Thus, estuarine nitrate has complex controls dictated by many factors, including the heterogeneity of sources, that require different monitoring strategies than for estuarine fDOM with watershed DOC.

Direct point-source inputs to the estuary likely do not vary considerably during storm events because of the absence of major combined sewer overflows in this watershed (NHDES, 2009). However, hydrodynamics may change during freshwater pulses (Zorndt et al., 2012) so the relative importance of point and non-point sources from different parts of the watershed may confound the estuarine signal. This also is apparent in the coherence response, where storm-event time scale coherence between watershed inputs and estuarine nitrate is greatly reduced, when compared with fDOM and Cl. This rapid dissipation of (the monitored) watershed NO₃ compared to terrestrial DOC signal in estuary has been observed elsewhere (Mooney & McClelland, 2012). Unraveling causes behind this divergence in NO₃ (compared to DOC and Cl) is centrally important for management, as it would suggest a need to focus on reducing point or non-point sources, or alternatively, develop a better understanding the internal fate of estuarine NO₃.

Estuaries are thought to be important net transformers of nitrate along the continuum from terrestrial uplands to



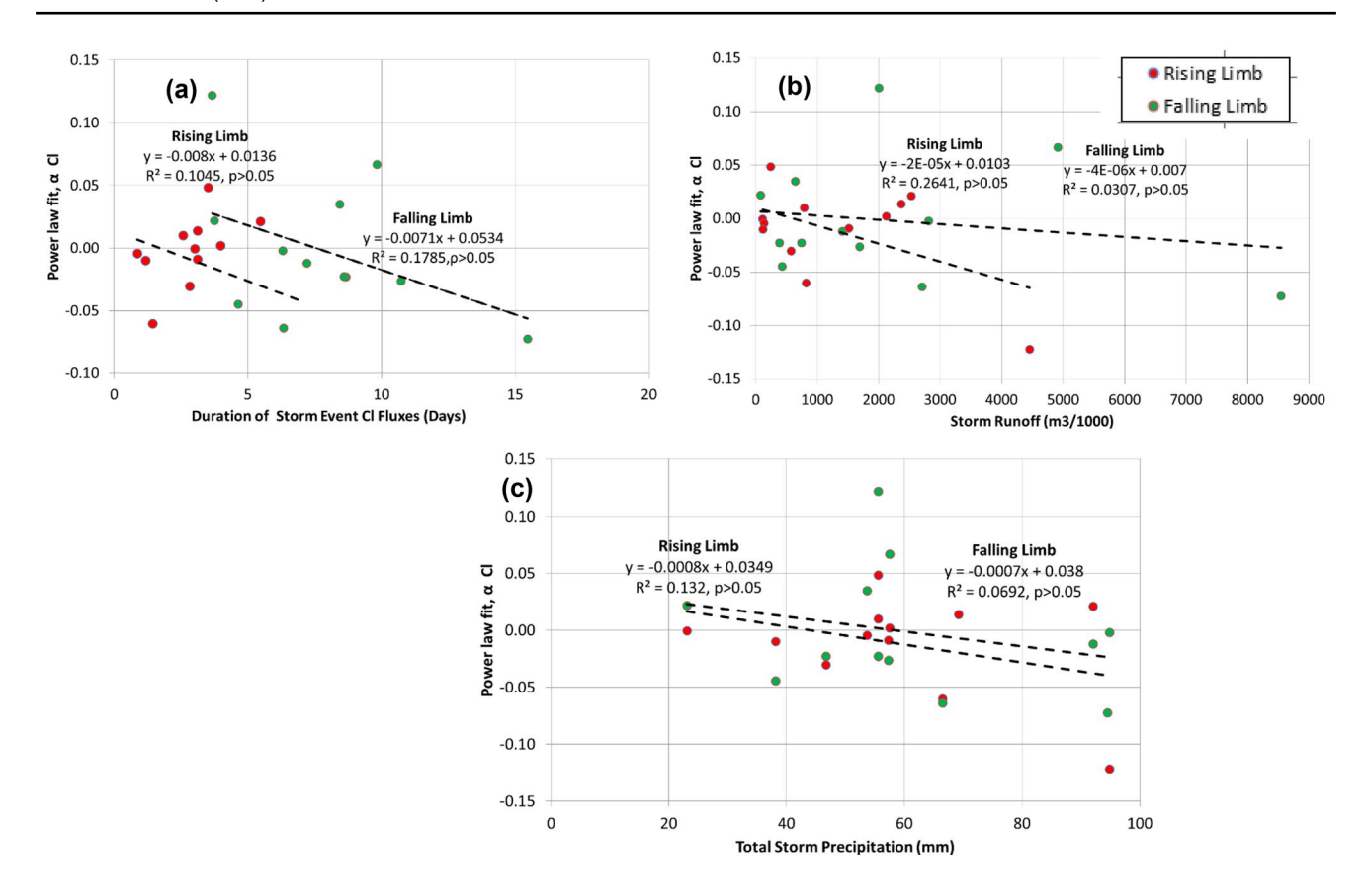


Fig. 9 Relationship between estuarine responsiveness (α) for Cl with (a) storm event duration, (b) total storm runoff, and (c) total storm precipitation

the open ocean (Galloway et al., 2003; Seitzinger et al., 2006). Net NO₃ removal during individual storm events could occur because of assimilation by macrophytes or algae, or via denitrification (Giblin et al., 2010; Kalnejais et al., 2007). The minimal response of NO₃ observed during intense late-summer storm events may be a result of internal estuarine processes resulting from warmer water (Hou et al., 2012; Ogilvie et al., 1997) (Fig. 5c). The effectiveness of removal of watershed inputs will vary depending on distance traveled from location of watershed input and estuarine measurement location. In addition, catchment characteristics that contribute to the quantity and timing of storm flows exported from watersheds may also a

play a role in the estuarine response. Geomorphology and basin geometry can control the shape and peak timing of storm hydrographs (Sólyom, 2004), whereas storm-event constituent concentrations are influenced by the spatial distribution of source materials (Walling & Webb, 1980), leading to the formation of hotspots of reactivity, that play an important role in processing of nitrogen (Mineau et al., 2015). It is likely that similar modifications also occur in estuaries. These observations, taken together with the coherence response, suggest that nitrate is spatially complex, underscoring the need for more expansive coupled biogeochemical monitoring of watersheds and their downstream estuaries over multiple growing seasons.

Table 3 Average coherence values over time scales larger than a day

	Watersh	Watershed variable							
Estuarine constituent	Q	NO ₃	DOC	Cl	NO ₃ flux	DOC flux	Cl flux		
NO ₃	0.21	0.049			0.133				
fDOM	0.217		0.087			0.208			
Cl	0.171			0.107			0.157		

Empty cells indicates no data



Conclusions

The use of simultaneous watershed-estuary measurements is a potentially powerful way to enhance understanding of estuarine conditions. It was exemplified here using continuous time series data and application of unique analysis techniques to examine temporal signatures of variability in estuarine nitrate and DOC and in the context of their watershed delivery mechanisms. Watershed control of nitrate and DOC was found to be strong in the baseflow-dominant seasonal and longer time scales. However, strong differences were revealed in intermediate, storm-event time scales, with DOC exhibiting stronger watershed connectivity, and nitrate showing complex patterns.

Although the near-conservative behavior of DOC was attributable to the relatively homogenous distribution of sources, a combination of factors led to the complex behavior of nitrate. Among them, sporadic distribution of sources, point-source dominance during baseflow, nonpoint source dominance with rapid depletion during storm events, and the high reactivity of nitrate (e.g., assimilatory and dissimilatory processes) could all contribute to the complex behavior of NO₃. Due to this homogenous nature of DOC sources, spatially limited but representative monitoring of DOC would be sufficient to capture its dynamics in the estuary. However, for nitrate, automated, appropriately scaled, sensor-based monitoring would be essential to meet the spatial resolution necessary in this watershed, and other impaired watersheds, where human activities have resulted in the formation of a heterogenous patches of sources and sinks. Such monitoring programs would need to be integrated with estuarine hydrodynamic models (Ganju et al., 2016) with input of high-resolution data of multiple elements (here DOC, Cl, and NO₃) to understand the spatially and temporally complex patterns (e.g., Testa et al., 2014). With human and climate-driven alterations of coastal ecosystems continuing to occur automated, simultaneous watershed-estuary biogeochemical measurements are essential, not only to develop targeted and effective nutrient-management activities but also to understand and predict climate-driven changes to exports of nutrients and carbon to the coastal waters.

Supplementary Information The online version contains supplementary material available at https://doi.org/10.1007/s12237-021-00965-8.

Acknowledgements We thank the editors and two anonymous reviewers for their insightful comments. This research was funded in part by National Science Foundation grants EPS 1101245 and OCE 1637630 (Plum Island Ecosystem LTER), NH Sea Grant (NOAA NA10OAR4170082), NH Agricultural Experiment Station, and UNH ESRC's Iola Hubbard Endowment for Climate Change. This is AES Scientific Contribution Number 2675 supported by the USDA NIFA Hatch Project 0225006. Raw data underlying this work is provided with the supporting information. Code related to the use of *frequency-dependent coherence* is available upon request.



- Arndt, S., Vanderborght, J. P., and Regnier, P. 2007. Diatom growth response to physical forcing in a macrotidal estuary: coupling hydrodynamics, sediment transport, and biogeochemistry. *Journal* of Geophysical Research: Oceans 112 (5). https://doi.org/10.1029/ 2006JC003581
- Balch, W., T. Huntington, G. Aiken, D. Drapeau, B. Bowler, L. Lubelczyk, and K. Butler. 2016. Toward a quantitative and empirical dissolved organic carbon budget for the Gulf of Maine, a semienclosed shelf sea. Global Biogeochemical Cycles 30 (2): 268–292. https://doi.org/10.1002/2015GB005332.
- Barbier, E.B., S.D. Hacker, C. Kennedy, E.W. Koch, A.C. Stier, and B.R. Silliman. 2011. The value of estuarine and coastal ecosystem services. *Ecological Monographs* 81 (2): 169–193. https://doi.org/10.1890/10-1510.1.
- Basu, N.B., G. Destouni, J.W. Jawitz, S.E. Thompson, N.V. Loukinova, A. Darracq, et al. 2010. Nutrient loads exported from managed catchments reveal emergent biogeochemical stationarity. *Geophysical Research Letters* 37 (23): 1–5. https://doi.org/10.1029/ 2010GL045168.
- Battin, T.J., L. a. Kaplan, S. Findlay, C.S. Hopkinson, E. Marti, A.I. Packman, et al. 2009. Biophysical controls on organic carbon fluxes in fluvial networks. *Nature Geoscience* 2 (8): 595–595. https://doi.org/10.1038/ngeo602.
- Bauer, J.E., W.-J. Cai, P.A. Raymond, T.S. Bianchi, C.S. Hopkinson, and P.A.G. Regnier. 2013. The changing carbon cycle of the coastal ocean. *Nature* 504 (7478): 61–70. https://doi.org/10.1038/ nature12857.
- Beem, N.T., and F.T. Short. 2009. Subtidal eelgrass declines in the Great Bay Estuary, New Hampshire and Maine, USA. *Estuaries and Coasts* 32 (1): 202–205. https://doi.org/10.1007/s12237-008-9110-3.
- Bergamaschi, B.A., J.A. Fleck, B.D. Downing, E. Boss, B.A. Pellerin, N.K. Ganju, et al. 2012a. Mercury dynamics in a San Francisco estuary tidal wetland: assessing dynamics using in situ measurements. *Estuaries and Coasts* 35 (4): 1036–1048. https://doi.org/ 10.1007/s12237-012-9501-3.
- Bergamaschi, B.A., D.P. Krabbenhoft, G.R. Aiken, E. Patino, D.G. Rumbold, and W.H. Orem. 2012b. Tidally driven export of dissolved organic carbon, total mercury, and methylmercury from a mangrove-dominated estuary. *Environmental Science and Technology* 46 (3): 1371–1378. https://doi.org/10.1021/es2029137.
- Bowen, J.L., and I. Valiela. 2008. N to assess coupling between watersheds and estuaries in temperate and tropical regions. *Journal of Coastal Research* 243 (243): 804–813. https://doi.org/10.2112/05-0545.1.
- Boyer, E.W., C.L. Goodale, N.A. Jaworski, and R.W. Howarth. 2002. Anthropogenic nitrogen sources and relationships to riverine nitrogen export in the northeastern U.S.A. *Biogeochemistry* 57–58: 137–169. https://doi.org/10.1023/A:1015709302073.
- Bresler, S.E. 2012. Policy recommendations for reducing reactive nitrogen from wastewater treatment in the Great Bay Estuary, NH. *Environmental Science and Policy* 19–20: 69–77. https://doi.org/10.1016/j.envsci.2012.02.006.
- Bricker, S.B., B. Longstaff, W. Dennison, A. Jones, K. Boicourt, C. Wicks, and J. Woerner. 2008. Effects of nutrient enrichment in the nation's estuaries: a decade of change. *Harmful Algae* 8 (1): 21–32. https://doi.org/10.1016/j.hal.2008.08.028.
- Buffam, I., Galloway, J. N., and Blum, L. K. 2001. A storm ow/base ow comparison of dissolved organic matter concentrations and bioavailability in an Appalachian stream. *Biogeochemistry* 269–306.
- Camporese, M., D. Penna, M. Borga, and C. Paniconi. 2014. A field and modeling study of nonlinear storage-discharge dynamics for an Alpine headwater catchment. Water Resources Research 50 (2): 806–822. https://doi.org/10.1002/2013WR013604.



- Carey, R.O.R.O., W.M.W.M. Wollheim, G.K.G.K. Mulukutla, and M.M.M.M. Mineau. 2014. Characterizing storm-event nitrate fluxes in a fifth order suburbanizing watershed using in situ sensors. *Environmental Science and Technology* 48 (14): 7756–7765. https://doi.org/10.1021/es500252j.
- Clair, T.A., I.F. Dennis, and S. Bélanger. 2013. Riverine nitrogen and carbon exports from the Canadian landmass to estuaries. *Biogeochemistry* 115 (1–3): 195–211. https://doi.org/10.1007/s10533-013-9828-2.
- Cloern, J.E., and F.H. Nichols. 1985. Time scales and mechanisms of estuarine variability, a synthesis fromstudies of San Francisco Bay. *Hydrobiologia* 12: 229–237.
- Coble, A.A., L.E. Koenig, J.D. Potter, L.M. Parham, and W.H. McDowell. 2019. Homogenization of dissolved organic matter within a river network occurs in the smallest headwaters. *Biogeochemistry* 143 (1): 85–104. https://doi.org/10.1007/s10533-019-00551-y.
- Colombo, M.J., S.J. Grady, and E. Trench. 2004. Nutrient enrichment, phytoplankton algal growth, and estimated rates of instream metabolic processes in the Quinebaug River Basin, Connecticut. Scientific Investigations Report 2000–2001: 2004–5227.
- Creed, I.F., S.E. Sanford, F.D. Beall, L.A. Molot, and P.J. Dillon. 2003. Cryptic wetlands: integrating hidden wetlands in regression models of the export of dissolved organic carbon from forested landscapes. *Hydrological Processes* 17 (18): 3629–3648. https://doi.org/10.1002/hyp.1357.
- Deegan, L. a., D.S. Johnson, R.S. Warren, B.J. Peterson, J.W. Fleeger, S. Fagherazzi, and W.M. Wollheim. 2012. Coastal eutrophication as a driver of salt marsh loss. *Nature* 490 (7420): 388–392. https://doi.org/10.1038/nature11533.
- Douglas, E.M., M. Asce, and C.A. Fairbank. 2011. Is precipitation in northern New England becoming more extreme? Statistical analysis of extreme rainfall in Massachusetts, New Hampshire, and Maine and updated estimates of the 100-year storm. *Most* 16 (3): 203–218. https://doi.org/10.1061/(ASCE)HE.1943-5584.0000303.
- Downing, B.D., B.a. Pellerin, B.a. Bergamaschi, J.F. Saraceno, and T.E.C. Kraus. 2012. Seeing the light: the effects of particles, dissolved materials, and temperature on in situ measurements of DOM fluorescence in rivers and streams. *Limnology and Ocean*ography: Methods 10: 767–775. https://doi.org/10.4319/lom.2012. 10.767.
- Dusek, J., and T. Vogel. 2016. Hillslope-storage and rainfall-amount thresholds as controls of preferential stormflow. *Journal of Hydrology* 534: 590–605. https://doi.org/10.1016/j.jhydrol.2016.01.047.
- Evans, C., and T.D. Davies. 1998. Causes of concentration/discharge hysteresis and its potential as a tool for analysis of episode hydrochemistry. *Water Resources Research* 34 (1): 129. https://doi.org/10.1029/97WR01881.
- Feinson, L.S., J. Gibs, T.E. Imbrigiotta, and J.D. Garrett. 2016. Effects of land use and sample location on nitrate-stream flow hysteresis descriptors during storm events. *Journal of the American Water Resources Association* 52 (6): 1493–1508. https://doi.org/10. 1111/1752-1688.12477.
- Galloway, J.N., J.D. Aber, J.W. Erisman, S.P. Seitzinger, R.W. Howarth, E.B. Cowling, and B.J. Cosby. 2003. The nitrogen cascade. *American Institute of Biological Sciences* 53 (4): 341. https://doi.org/10.1641/0006-3568(2003)053[0341:TNC]2.0.CO;2.
- Ganju, N.K., J.L. Miselis, and A.L. Aretxabaleta. 2014. Physical and biogeochemical controls on light attenuation in a eutrophic, backbarrier estuary. *Biogeosciences* 11 (24): 7193–7205. https://doi. org/10.5194/bg-11-7193-2014.
- Ganju, N.K., M.J. Brush, B. Rashleigh, A.L. Aretxabaleta, P. del Barrio, J.S. Grear, et al. 2016. Progress and challenges in coupled hydrodynamic-ecological estuarine modeling. *Estu*aries and Coasts 39 (2): 311–332. https://doi.org/10.1007/ s12237-015-0011-y.

- Giblin, A.E., N.B. Weston, G.T. Banta, J. Tucker, and C.S. Hopkinson. 2010. The effects of salinity on nitrogen losses from an oligohaline estuarine sediment. *Estuaries and Coasts* 33 (5): 1054–1068. https://doi.org/10.1007/s12237-010-9280-7.
- Gilbert, M., J. Needoba, C. Koch, A. Barnard, and A. Baptista. 2013. Nutrient loading and transformations in the Columbia River estuary determined by high-resolution in situ sensors. *Estuaries and Coasts* 36 (4): 708–727. https://doi.org/10.1007/ s12237-013-9597-0.
- Godsey, S.E., J.W. Kirchner, and D.W. Clow. 2009. Concentrationdischarge relationships reflect chemostatic characteristics of US catchments. *Hydrological Processes* 23 (13): 1844–1864. https:// doi.org/10.1002/hyp.7315.
- Grabowski, J., & Peterson, C. 2007. Restoring oyster reefs to recover ecoystem services. *Ecosystem Engineers: From Plants to Protists*, 405. Retrieved from http://books.google.com/books?id= Kg8sPBi8XnYC&printsec=frontcover
- Hanley, K.W., Wollheim, W.M., Salisbury, J., Huntington, T., and Aiken, G. 2013. Controls on dissolved organic carbon quantity and chemical character in temperate rivers of North America. *Global Biogeochemical Cycles* 27 (2): 492–504. https://doi.org/ 10.1002/gbc.20044
- Hayhoe, K., C.P. Wake, T.G. Huntington, L. Luo, M.D. Schwartz, J. Sheffield, et al. 2007. Past and future changes in climate and hydrological indicators in the US Northeast. *Climate Dynamics* 28 (4): 381–407. https://doi.org/10.1007/s00382-006-0187-8.
- Hou, L., M. Liu, S.A. Carini, and W.S. Gardner. 2012. Transformation and fate of nitrate near the sediment-water interface of Copano Bay. *Continental Shelf Research* 35: 86–94. https://doi.org/10.1016/j.csr.2012.01.004.
- Huang, W., Hagen, S., and Bacopoulos, P. 2014. Hydrodynamic modeling of Hurricane Dennis impact on estuarine salinity variation in Apalachicola Bay. *Journal of Coastal Research* 389–398.https://doi.org/10.2112/JCOASTRES-D-13-00022.1
- Jiang, Y., Frankenberger, J.R., Bowling, L.C., and Sun, Z. 2014. Quantification of uncertainty in estimated nitrate-N loads in agricultural watersheds. *Journal of Hydrology* 519 (PA): 106–116. https://doi.org/10.1016/j.jhydrol.2014.06.027
- Johnson, K.S., L.J. Coletti, and F.P. Chavez. 2006. Diel nitrate cycles observed with in situ sensors predict monthly and annual new production. *Deep-Sea Research Part I: Oceanographic Research Papers* 53 (3): 561–573. https://doi.org/10.1016/j.dsr.2005.12. 004.
- Kaller, M.D., R.F. Keim, B.L. Edwards, A. Raynie Harlan, T.E. Pasco, W.E. Kelso, and D. Allen Rutherford. 2015. Aquatic vegetation mediates the relationship between hydrologic connectivity and water quality in a managed floodplain. *Hydrobiologia* 760 (1): 29–41. https://doi.org/10.1007/s10750-015-2300-7.
- Kalnejais, L.H., W.R. Martin, R.P. Signell, and Michael H. Bothner. 2007. Role of sediment resuspension in the remobilization of particulate-phase metals from coastal sediments. *Environmental Science & Technology* 41 (7): 2282–2288. https://doi.org/10.1021/es061770z.
- Kaushal, S.S., W.H. McDowell, and W.M. Wollheim. 2014. Tracking evolution of urban biogeochemical cycles: past, present, and future. *Biogeochemistry* 121 (1): 1–21. https://doi.org/10.1007/s10533-014-0014-y.
- Koenig, L. E., Shattuck, M. D., Snyder, L. E., Potter, J. D., & McDowell, W. H. 2017. Deconstructing the effects of flow on DOC, nitrate, and major ion interactions using a high-frequency aquatic sensor network. Water Resources Research 53 (12): 10655–10673. https://doi.org/10.1002/2017WR020739
- Larsen, L., J. Harvey, K. Skalak, and M. Goodman. 2015. Fluorescence-based source tracking of organic sediment in restored and unrestored urban streams. *Limnology and Oceanography* 60 (4): 1439–1461. https://doi.org/10.1002/lno.10108.



- Lloyd, C.E.M., J.E. Freer, P.J. Johnes, and A.L. Collins. 2016. Using hysteresis analysis of high-resolution water quality monitoring data, including uncertainty, to infer controls on nutrient and sediment transfer in catchments. Science of the Total Environment 543: 388–404. https://doi.org/10.1016/j.scitotenv.2015.11.028.
- Mantoura, R.F.C., and E.M.S. Woodward. 1983. Conservative behaviour of riverine dissolved organic carbon in the Severn Estuary: chemical and geochemical implications. *Geochimica Et Cosmochimica Acta* 47 (7): 1293–1309. https://doi.org/10.1016/0016-7037(83)90069-8.
- McClelland, J.W., and I. Valiela. 1998. Linking nitrogen in estuarine producers to land-derived sources. *Limnology and Oceanogra*phy 43 (4): 577–585. https://doi.org/10.4319/lo.1998.43.4.0577.
- McKenna, J. 2004. DOC dynamics in a small temperate estuary: simultaneous addition and removal processes and implications on observed nonconservative behavior. *Estuaries* 27 (4): 604–616. https://doi.org/10.1007/BF02907648.
- Menke, W., and J. Menke. 2012. Environmental data analysis with MatLab. *Environmental Data Analysis with MatLab*. https://doi.org/10.1016/B978-0-12-391886-4.00012-X.
- Mills, K. 2009. Ecological trends in the Great Bay estuary. Durham, NH. Retrieved from http://greatbay.org/documents/20th-gbnerr-report.pdf
- Mineau, M.M., W.M. Wollheim, and R.J. Stewart. 2015. An index to characterize the spatial distribution of land use within watersheds and implications for river network nutrient removal and export. *Geophysical Research Letters* 42 (16): 6688–6695. https://doi.org/10.1002/2015GL064965.
- Mooney, R. F., and McClelland, J. W. 2012. Watershed export events and ecosystem responses in the mission—Aransas National Estuarine Research Reserve, South Texas. *Estuaries and Coasts* 1–18. https://doi.org/10.1007/s12237-012-9537-4
- Moran, M.A., W.M. Sheldon, and J.E. Sheldon. 1999. Biodegradation of riverine dissolved organic carbon in five estuaries of the southeastern United States. *Estuaries* 22 (1): 55. https://doi.org/10.2307/1352927.
- Morse, N.B., and W.M. Wollheim. 2014. Climate variability masks the impacts of land use change on nutrient export in a suburbanizing watershed. *Biogeochemistry* 121 (1): 45–59. https://doi.org/10.1007/s10533-014-9998-6.
- NHDES. 2009. Combined sewer overflows in New Hampshire. An NH Department of Environmental Services Factsheet. [Online]. Concord, NH. https://doi.org/10.1016/S0273-1223(98)00802-6
- Nippgen, F., B.L. McGlynn, and R.E. Emanuel. 2015. The spatial and temporal evolution of contributing areas. *Water Resources Research* 51 (6): 4550–4573. https://doi.org/10.1002/2014W R016719
- O'Boyle, S., P. Trickett, A. Partington, and C. Murray. 2014. Field testing of an optical in situ nitrate sensor in three Irish estuaries. *Biology and Environment* 114 (1): 3318. https://doi.org/10.3318/BIOE.2014.02.
- Ogilvie, B., D.B. Nedwell, R.M. Harrison, A. Robinson, and A. Sage. 1997. High nitrate, muddy estuaries as nitrogen sinks: the nitrogen budget of the River Colne estuary (United Kingdom). *Marine Ecology Progress Series* 150 (1–3): 217–228. https://doi.org/10.3354/meps150217.
- Phillips, J.D. 2003. Sources of nonlinearity and complexity in geomorphic systems. *Progress in Physical Geography* 27 (1): 1–23. https://doi.org/10.1191/0309133303pp340ra.
- Pinckney, J.L., H.W. Paerl, P. Tester, and T.L. Richardson. 2001. The role of nutrient loading and eutrophication in estuarine ecology. *Environmental Health Perspectives* 109 (SUPPL. 5): 699–706. https://doi.org/10.1289/ehp.01109s5699.
- PREP. 2013. State of our estuaries 2013, 48. https://doi.org/10.2217/pmt.13.66

- Raymond, P.A., and J.E. Saiers. 2010. Event controlled DOC export from forested watersheds. *Biogeochemistry* 100 (1): 197–209. https://doi.org/10.1007/s10533-010-9416-7.
- Raymond, P. A., and Spencer, R. G. M. 2014. Riverine DOM. In Biogeochemistry of Marine Dissolved Organic Matter: Second Edition (pp. 509–533).https://doi.org/10.1016/B978-0-12-405940-5.00011-X
- Robins, P.E., M.J. Lewis, J. Freer, D.M. Cooper, C.J. Skinner, and T.J. Coulthard. 2018. Improving estuary models by reducing uncertainties associated with river flows. *Estuarine*, *Coastal and Shelf Science* 207: 63–73. https://doi.org/10.1016/j.ecss.2018.02.015.
- Salisbury, J.E., D. Vandemark, C.W. Hunt, J.W. Campbell, W.R. McGillis, and W.H. McDowell. 2008. Seasonal observations of surface waters in two Gulf of Maine estuary-plume systems: relationships between watershed attributes, optical measurements and surface pCO₂. Estuarine, Coastal and Shelf Science 77 (2): 245–252. https://doi.org/10.1016/j.ecss.2007.09.033.
- Salisbury, J.E., D. Vandemark, C. Hunt, J. Campbell, B. Jonsson, A. Mahadevan, et al. 2009. Episodic riverine influence on surface DIC in the coastal Gulf of Maine. *Estuarine, Coastal and Shelf Science* 82 (1): 108–118. https://doi.org/10.1016/j.ecss.2008.12.021.
- Saraceno, J.F., B.A. Pellerin, B.D. Downing, E. Boss, P.A.M. Bachand, and B.A. Bergamaschi. 2009. High-frequency in situ optical measurements during a storm event: assessing relationships between dissolved organic matter, sediment concentrations, and hydrologic processes. *Journal of Geophysical Research: Biogeosciences* 114 (4): 1–11. https://doi.org/10.1029/2009JG000989.
- Schlesinger, W. H., and Bernhardt, E. S. 2013. Chapter 5—the biosphere: the carbon cycle of terrestrial ecosystems. In W. H. Schlesinger & E. S. Bernhardt (Eds.), *Biogeochemistry (Third Edition)* (Third Edit, pp. 135–172). Boston: Academic Press. https://doi.org/10.1016/B978-0-12-385874-000005-4
- Seitzinger, S.P., and C. Kroeze. 1998. Global distribution of nitrous oxide production and n inputs in freshwater and coastal marine ecosystems. *Global Biogeochemical Cycles* 12 (1): 93–113. https://doi.org/10.1029/97GB03657.
- Seitzinger, S.P., J.A. Harrison, J.K. Bohlke, A.F. Bouwman, R. Lowrance, B. Peterson, et al. 2006. Denitrification across landscapes and waterscapes: a synthesis. *Ecological Applications*. https://doi.org/10.1890/1051-0761(2006)016[2064:DALAWA]2.0.CO;2.
- Short, F. T. 1992. The ecology of the Great Bay Estuary, New Hampshire and Maine: an estuarine profile and bibliography.
- Smyth, A.R., S.P. Thompson, K.N. Siporin, W.S. Gardner, M.J. McCarthy, and M.F. Piehler. 2013. Assessing nitrogen dynamics throughout the estuarine landscape. *Estuaries and Coasts* 36 (1): 44–55. https://doi.org/10.1007/s12237-012-9554-3.
- Sólyom, P.B. 2004. Effect of limited storm duration on landscape evolution, drainage basin geometry, and hydrograph shapes. *Journal of Geophysical Research* 109 (F3): F03012. https://doi.org/10.1029/2003JF000032.
- Statham, P.J. 2012. Nutrients in estuaries—an overview and the potential impacts of climate change. *Science of the Total Environment* 434: 213–227. https://doi.org/10.1016/j.scitotenv.2011.09.088.
- Swaney, D.P., D. Scavia, R.W. Howarth, and R.M. Marino. 2008. Estuarine classification and response to nitrogen loading: insights from simple ecological models. *Estuarine, Coastal and Shelf Science* 77 (2): 253–263. https://doi.org/10.1016/j.ecss.2007.09.013.
- Testa, J.M., Y. Li, Y.J. Lee, M. Li, D.C. Brady, D.M. Di. Toro, et al. 2014. Quantifying the effects of nutrient loading on dissolved O₂ cycling and hypoxia in Chesapeake Bay using a coupled hydrodynamic-biogeochemical model. *Journal of Marine Systems* 139 (March): 139–158. https://doi.org/10.1016/j.jmarsys.2014.05.018.
- Traving, S.J., O. Rowe, N.M. Jakobsen, H. Sørensen, J. Dinasquet, C.A. Stedmon, et al. 2017. The effect of increased loads of dissolved organic matter on estuarine microbial community composition and



- function. Frontiers in Microbiology 8 (351): 1–15. https://doi.org/10.3389/fmicb.2017.00351.
- Trowbridge, P. 2010. Analysis of nitrogen loading reductions for waste-water treatment facilities and non-point sources in the Great Bay estuary watershed. Concord, NH. Retrieved from http://des.nh.gov/organization/divisions/water/wmb/coastal/documents/gb_nitro_load_analysis.pdf
- Trowbridge, P., Wood, M., Underhill, J., and Healy, D. 2014. *Great Bay nitrogen non-point source study. State of New Hampshire, Department of Environmental Services*. 82pp. Retrieved from https://scholars.unh.edu/prep/381/
- Valiela, I., and J.L. Bowen. 2002. Nitrogen sources to watersheds and estuaries: role of land cover mosaics and losses within watersheds. *Environmental Pollution* 118 (2): 239–248. https://doi.org/10.1016/S0269-7491(01)00316-5.
- Vallino, J.J., C.S. Hopkinson, and R.H. Garritt. 2005. Estimating estuarine gross production, community respiration and net ecosystem production: a nonlinear inverse technique. *Ecological Modelling* 187 (2–3): 281–296. https://doi.org/10.1016/j.ecolmodel.2004.10.018.
- Walling, D. E., and Webb, B. W. 1980. The spatial dimension in the interpretation of stream solute behaviour. *Journal of Hydrology* 47 (1): 129–149. https://doi.org/10.1016/0022-16948090052-9

- Wetz, M.S., and D.W. Yoskowitz. 2013. An "extreme" future for estuaries? Effects of extreme climatic events on estuarine water quality and ecology. *Marine Pollution Bulletin* 69 (1): 7–18.
- Williams, G.P. 1989. Sediment concentration versus water discharge during single hydrologic events in rivers. *Journal of Hydrology* 111 (1–4): 89–106. https://doi.org/10.1016/0022-1694(89) 90254-0.
- Wollheim, W.M., B.A. Pellerin, C.J. Vörösmarty, and C.S. Hopkinson. 2005. N retention in urbanizing headwater catchments. *Ecosystems* 8 (8): 871–884. https://doi.org/10.1007/s10021-005-0178-3.
- Wollheim, W. M., Stewart, R. J., Aiken, G. R., Butler, K. D., Morse, N. B., and Salisbury, J. 2015. Removal of terrestrial DOC in aquatic ecosystems of a temperate river network. *Geophysical Research Letters* 42 (16): 6671–6679. https://doi.org/10.1002/2015GL064647
- Zorndt, A. C., Schlurmann, T., and Grabemann, I. 2012. The influence of extreme events on hydrodynamics and salinities in the Weser Estuary in the context of climate impact research. *Coastal Engineering Proceedings* (33): 1–12. https://doi.org/10.9753/icce.v33.currents.50

